



## Frequency and amplitude tracking for short nonstationary and nonlinear signals

### Keynote address

**Nadine Martin**

**Michelle Vieira**

GIPSA-lab, INPG/CNRS  
Department Images Signal  
Grenoble Campus  
BP 46 - 961, rue de la Houille Blanche  
F-38402 Saint Martin d'Hères – France

[nadine.martin@gipsa-lab.inpg.fr](mailto:nadine.martin@gipsa-lab.inpg.fr)

[michelle.vieira@gipsa-lab.inpg.fr](mailto:michelle.vieira@gipsa-lab.inpg.fr)

### ABSTRACT

Whatever the application domains, when dealing with strongly nonstationary and nonlinear signals, Fourier-based methods and even classical time-frequency methods are no longer able to estimate and track the instantaneous amplitudes and frequencies of each signal component. One possibility to get away from the Heisenberg uncertainty constraint is to set a model, which has to be as general as possible in order to be valid in many domains. In that context, we have proposed and studied a new model, which writes as a time-varying polynomial-amplitude and polynomial-phase signal. Parameter estimation is casted as the maximisation of the likelihood function, which is overcome by meta-heuristic approaches, such as simulating annealing. In that paper, based on simulations, we detail the performance of the Short Local Polynomial model-based method (Short-LP) we proposed for a number of particular cases when analysing one or two components on very short-time duration. We first assess the frequency resolution limit when analysing close frequency-modulated components. The performance is explained according to classical Fourier limits and more particularly the dynamic signal bandwidth, the signal being nonstationary. The analysis of amplitude-modulated components is then discussed according to the presence or not of the carrier frequency. Finally, we stress upon the performance of the amplitude estimation in the particular case where the instantaneous frequencies are known *a priori*.

### KEYWORDS

Signal processing, time-frequency, nonstationary, instantaneous frequency and amplitude, polynomial phase signal, simulating annealing, tracking.

## I. INTRODUCTION

Surveillance is based on indicator monitoring. When an indicator exceeds a threshold, an alarm is raised. An absolute threshold on scalar indicators is the most widespread approach but is not adapted to the detection of some damages. For instance in rotating machines, unbalances, misalignments, anisotropic rotors, flexible coupling or magnetic bearings infer excitation forces, which amplitude and frequency are modulated. In that case, typological indicators are essential for a reliable and early detection. A highly evolved indicator is capable to directly represent the vibration image of a default and to track its evolution.

A time model of a measure provides an accurate description of this observation, which parameters can be such typological indicators. In previous publications [3-4-5-6-7-8-9], we have proposed a time model for signals having strong nonstationarities. Furthermore this model based on a Short Local Polynomial model (Short-LP) is relevant for processing short signals. In all the methods belonging to the Cohen class, the resolution is limited by the Heisenberg uncertainty. To get away from this constraint and to be able to estimate nonlinear modulated signals with a better resolution need to add some hypothesis mostly if the signal analysis is of short duration.

We will not handle the statistical properties of the Short-LP estimator proposed, this topic has been thoroughly covered in previous publications [3-4]. We will now focus on some important issues for the analysis of multicomponent signals.

Based on simulations, we detail the performance of the algorithm for a number of particular cases when analysing components on very short-time duration. We first assess the frequency resolution limit when analysing close frequency-modulated components. The performance is explained according to classical Fourier limits and more particularly the dynamic signal bandwidth, the signal being nonstationary. The analysis of amplitude-modulated components is then discussed according to the presence or not of the carrier frequency. Finally, we stress upon the performance of the amplitude estimation in the particular case where the instantaneous frequencies are known *a priori*

This paper is outlined as follows. Section II will recall the model used for modelling short nonstationary signals. Section III briefly describes the optimization algorithms chosen to estimate the model parameters whereas section IV deals with the multicomponent case. The last sections present new results elaborated for a number of simulated signals in order to highlight important properties of the algorithm proposed: the frequency resolution limit in section V, the behaviour of the algorithm face to amplitude modulation without carrier in section VI and the improve of performance with prior upon frequency modulation in section VII. Section VIII looks at the conclusions that can be drawn from this work.

## II. THE MODEL WITH A SPECIFIC BASE

Let us consider a model  $x[n]$  of a discrete signal defined as the sum of  $C$  components  $x_c[n]$ ,

$$x[n] = \sum_{c=1}^C x_c[n], \quad (1)$$

$$\text{with } x_c[n] = a_c[n] \cos(\phi_c[n]) \quad \text{and} \quad n = -N/2, N/2,$$

where amplitudes  $a_c[n]$  are strictly positive, phases  $\phi_c[n]$  are differentiable and show no discontinuity. The constraint on the amplitudes and the phases guaranty the unicity of the model [2, 10].

A way of modelling the signal with a better accuracy is to increase the number of parameters to describe it without being over the point number of the signal. In [3], we propose a polynomial modelling of each amplitude  $a_c[n]$  and of each frequency  $f_c[n]$ . The phases  $\phi_c[n]$  of each component are then obtained by a discrete integration of  $f_c[n]$  up to  $2\pi$ . For each  $c$  varying from 1 to  $C$ , the approximation is given by

$$\begin{aligned} a_c[n] &= \sum_{m=0}^{Ma_c} a_{c,m} p_m[n], \\ f_c[n] &= \sum_{m=0}^{Mf_c} f_{c,m} p_m[n], \\ \phi_c[n] &= \varphi_c + 2\pi \left( \sum_{k=-N/2}^n f_c[k] - \sum_{k=-N/2}^0 f_c[k] \right), \end{aligned} \quad (2)$$

where  $Ma_c$  and  $Mf_c$  are the approximation orders of the amplitude modulation and frequency modulation respectively.  $\varphi_c$  stands for the initial phase of the signal in (1).

The set  $\{p_m[n]\}_{m=0, \max(Ma_c, Mf_c)}$  is a polynomial base. This base could be computed from the discretization of a continuous-time base, such as the canonical polynomial base or the orthogonal polynomial bases, such as Legendre, Tchebychev or Hermite. However the orthogonal property is lost when discretizing these functions. This property is fundamental to guarantee the independence between the parameters estimated. Therefore, in Short-LP, we use a discrete base we derived in [3] and which corresponds to the application of the Gram Schmidt procedure in discrete-time directly. The expressions for the set  $\{p_m[n]\}_{m=0, \max(Ma_c, Mf_c)}$  are recall in Appendix.

Finally the parameters to estimate can be gathered in a vector  $\mathbf{V}$

$$\mathbf{V} = [\mathbf{V}_1^T \dots \mathbf{V}_C^T] \quad (3)$$

with

$$\mathbf{V}_c = [a_{c,0} \dots a_{c, Ma_c} \quad \varphi_c \quad f_{c,0} \dots f_{c, Mf_c}]^T \text{ with } c=1, C \quad (4)$$

The dimension of the vector  $\mathbf{V}$  is equal to  $C \times M$  with  $M = Ma_c + Mf_c + 3$ , the dimension of each vector  $\mathbf{V}_c$ .

In addition to the choice of the base, the choice of modelling the frequency instead of the phase and the centring of the polynomial at the signal middle to ensure a minimum variance, the idea was to also consider only small approximation orders in Short-LP [3].  $Ma_c$  and  $Mf_c$  are less than or equal to 2. This rule does not induce a constraint since the signal analysed is assumed to be short enough to be adapted to this approximation. The signal duration should contain one or two periods at least.

In order to generate the model (1), two approaches have been considered to estimate the vector  $\mathbf{V}$ . One possible approach is to consider the maximisation of the likelihood function, which is

equivalent to a minimization of the least square function  $l_{LS}(\mathbf{V})$  when the error can be assumed to be a Gaussian noise. This minimization is

$$\hat{\mathbf{V}} = \arg \min_{\mathbf{V}} l_{LS}(\mathbf{V}), \quad (5)$$

with

$$l_{LS}(\mathbf{V}) = \sum_{n=-N/2}^{N/2} |s[n] - x[n]|^2, \quad (6)$$

where  $s[n]$  is the observation and  $x[n]$  the model defined in (1). The error between the observation and the model, namely the difference  $(s[n] - x[n])$ , represents the sum of the noise, in which the deterministic signal we want to estimate is embedded, and the model error. We verify *a posteriori* that this error is distributed as a Gaussian law.

Direct minimization of (6) is extremely difficult due to the high non-linearity of the function and the parameter number. Classical optimization techniques such as gradient descent, Gauss-Newton and EM algorithm do not ensure convergence to the global minimum when local minima are numerous. This problem can be overcome with meta-heuristic approaches, and in particular, with the simulated annealing algorithm. The simulated annealing technique is efficiency, when a desired global extremum is hidden in many local extrema. The simulated annealing has an analogy with thermodynamics where metal cools and anneals. In the same way, after an initialization of the parameter vector to estimate, an iterative loop, controlled by a scalar referred to as a temperature, generates a new candidate of the vector that minimizes the cost function, namely the least square function  $l_{LS}(\mathbf{V})$ . This candidate is accepted or not according the acceptance Metropolis rule.

In lieu of a likelihood maximum approach, a second approach can also be investigated upon a Bayesian point of view. In that case, the parameters in  $\mathbf{V}$  and the variance of the error  $(s[n] - x[n])$  are viewed as random variables for which a prior distribution has to be assigned. A straightforward calculation leads to an expression of the posterior distribution up to a normalisation constant. This function being highly nonlinear, we propose to use a Metropolis-Hasting MCMC algorithm to sample from this distribution. Once this distribution is estimated, the parameters are estimated by a Minimum Mean Square Error method [3].

By comparing both estimation algorithms [3], we concluded that the simulating annealing approach, in addition to a simple implementation, has provided a better compromise between the bias and mean square errors of the parameter estimates and the computation time. In this paper, we will then only use the simulating annealing based approach with the Short-LP.

The method was extended to a monocomponent signal whatever its length and its modulations by considering a local approximation on nonsequential parts of the signal. This issue is not considered in this paper, the reader should refer to [4] for details about this extension.

### III. OPTIMIZATION TECHNIQUE FOR A MONOCOMPONENT SIGNAL

Let us come back to the approximation of a short monocomponent signal  $x_c[n]$  defined in (1). In that case only one vector  $\mathbf{V}_c$  of dimension  $M$ , as defined in (4), has to be estimated. Table 1 gives the tuning of the Short-LP running with a simulating annealing based algorithm.

<b>Inputs</b>	
- $s[n]$	the observation over $[N/2, N/2]$
- $Ma_c$	the order of the amplitude polynomial (by default 2)
- $Mf_c$	the order of the frequency polynomial (by default 2)
- $iter$	the number of iterations (by default 70 000)
- $p_B$	the Bernoulli-distribution parameter (by default 0.01)
- $\varepsilon_\sigma$	the decrement of the parameter perturbation variance (by default 0.01)
- $\varepsilon_\tau$	the decrement of the temperature (by default 0.01)
- $v_b$	a rough estimation of the additive noise variance
- $z_\alpha$	$\alpha$ -quantile for the Gaussian distribution (by default $\alpha=31\%$ and $z_\alpha=1$ )
<b>Step 1. Initialization</b>	
- $\mathbf{V}_c^{(0)} = [a_{c,0}^{(0)} \ 0 \dots 0 \ \phi_c^{(0)} \ f_{c,0}^{(0)} \ 0 \dots 0]^T$	the parameter vector with
$f_{c,0}^{(0)} = \arg \max_v  FT_{s_c}(f) $	$a_{c,0}^{(0)} =  FT_{s_c}(f_0^{(0)}) $ $\phi_c^{(0)} = \arg FT_{s_c}(f_0^{(0)})$ where $FT_{s_c}(f) = \sum_{n=-N/2}^{N/2} s_c[n] e^{-2\pi i f n}$
- $a_c^{(0)}[n] = \sum_{m=0}^{Ma_c} a_{c,m}^{(0)} p_m[n]$ , $f_c^{(0)}[n] = \sum_{m=0}^{Mf_c} f_{c,m}^{(0)} p_m[n]$ , $\phi_c^{(0)}[n] = \phi_c^{(0)} + 2\pi \left( \sum_{k=-N/2}^n f_c^{(0)}[k] - \sum_{k=-N/2}^0 f_c^{(0)}[k] \right)$	
- $x_c^{(0)}[n] = a_c^{(0)}[n] \cos(\phi_c^{(0)}[n])$	the model evaluated from $\mathbf{V}_c^{(0)}$
- $l_{LS}(\mathbf{V}_c^{(0)}) = \sum_{n=-N/2}^{N/2}  s[n] - x_c^{(0)}[n] ^2$	the LS function
- $\Sigma_M^{(0)} = \text{diag}(\sigma_{(i)}^{2(0)})$	the $M \times M$ diagonal matrix of the initial parameter perturbation, $\sigma_{(i)}^{2(0)}$ being the parameter variances (by default setting to $\max(s[n])$ for the amplitude parameters, $2\pi$ for the initial phase and half of the sampling frequency for the frequency parameters, these values being formulated in the chosen base)
- $\tau^{(0)} = l_{LS}(\mathbf{V}_c^{(0)})$	the initial temperature
<b>Step 2. Iterations from <math>t=1, iter</math></b>	
- Generate a new parameter vector deviated from a Gaussian perturbation	$\mathbf{V}_c^{(gen)} = \mathbf{V}_c^{(t)} + \delta \mathbf{V}_c^{(t)}$ with $\delta \mathbf{V}_c^{(t)} = \mathbf{N}(0, \Sigma_M^{(t)})$
- Compute the model from $\mathbf{V}_c^{(gen)}$	$x_c^{(gen)}[n] = a_c^{(gen)}[n] \cos(\phi_c^{(gen)}[n])$
- Compute the LS function	$l_{LS}(\mathbf{V}_c^{(gen)})$
- Draw a random number according to a uniform distribution	$u \sim U[0,1]$
- Apply the acceptance Metropolis rule	
If $u < \exp\left(\frac{l_{LS}(\mathbf{V}_c^{(t)}) - l_{LS}(\mathbf{V}_c^{(gen)})}{\tau^{(t)}}\right)$	set $\mathbf{V}_c^{(t+1)} = \mathbf{V}_c^{(gen)}$ , $l_{LS}(\mathbf{V}_c^{(t+1)}) = l_{LS}(\mathbf{V}_c^{(gen)})$
	otherwise $\mathbf{V}_c^{(t+1)} = \mathbf{V}_c^{(t)}$ , $l_{LS}(\mathbf{V}_c^{(t+1)}) = l_{LS}(\mathbf{V}_c^{(t)})$
- Draw a random number according to a Bernoulli distribution	$u \sim B(p_B)$
- If $u=1$	set $\sigma_{(i)}^{2(t+1)} = (1 - \varepsilon_\sigma) \sigma_{(i)}^{2(t)} \ \forall i$ and $\tau^{(t+1)} = (1 - \varepsilon_\tau) \tau^{(t)}$
	otherwise set $\sigma_{(i)}^{2(t+1)} = \sigma_{(i)}^{2(t)} \ \forall i$ and $\tau^{(t+1)} = \tau^{(t)}$
- While $t < iter$	set $t=t+1$ and <b>iterate step 2</b>
<b>Stop criterion</b>	
- If $\left  \left( e^{iter}[n] \right)^2 - v_b(N+1) \right  < z_\alpha \sqrt{v_b^2(N+1)}$	set $x_c[n]$ from $\widehat{\mathbf{V}}_c = \mathbf{V}_c^{(iter)}$ and <b>stop the algorithm</b>
	otherwise <b>repeat step 2</b>

Table 1 - The Short-LP with a simulating-annealing-based algorithm for a monocomponent signal

## IV. THE CASE OF MULTICOMPONENT SIGNALS

In the case of a multicomponent signal, which is the purpose of this paper, the model is always defined in (1) but with  $C > 1$ . The dimension of the parameter vector  $\mathbf{V}$ , equal to  $C \times M$ , is high and represents the dimension of the parameter space describing the signal. In order that the modelling makes sense, this dimension has to be lower than the degree of freedom of the signal. Subsequently, this dimension has to be lower than  $N+1$ , the length of the signal. We then deduce the largest number of components,

$$C \leq \frac{N+1}{M}, \quad (7)$$

that the model can take into account. This constraint is strong in the context of short signals with non-linear modulations in frequency and in amplitude. Namely, this means that for a classical modelling with polynomial functions of order 2,  $M$  is equal to 7 and the number of components cannot be greater than 4 for a signal length of 32 points. This strong limit is due to the high precision of the model, which, as we will see in the following, will induce high performance at the expense of the computation time.

In [6] and [7], two approaches have been considered for estimating the parameters.

The first is referred to as the global algorithm and is a direct generalization of the previous algorithm. All of the parameters of all the components are estimated together. The algorithm derived is then optimal regarding the maximum likelihood, but it is important to notice that this property is true asymptotically only.

The second one is a method by deflation, where the highest-energy component is first estimated, then extracted from the observation in order to estimate the following one. Due to its design, this algorithm is suboptimal but with a less computational time.

The two following sections sum up these two approaches by pointing out the steps modified with respect to the algorithm developed in the monocomponent case.

### 3.1. Global algorithm

The global algorithm is close to the one presented in Table 1. In the initialization step, named *step 1*, the parameter vector  $\mathbf{V}_c$  of each component is estimated by a deflation method applied on a Fourier transform, the number  $C$  of components being known. The perturbation matrix is now of dimension  $C \times M$  and is initialized in the same way.

In order to increase the convergence rate and to reduce the computational time, which can be very high according to the observations, the adaptation has consisted in reducing the random perturbation in the iteration *step 2* of Table 1.

Table 2 shows the new iteration step, referred to as *step 2'* where the Metropolis rule is no more applied.

**Step 2' - Iterations from  $t=1$ , iter**

- Generate a new parameter vector deviated from a Gaussian perturbation

$$\mathbf{V}^{(gen)} = \mathbf{V}^{(t)} + \delta\mathbf{V}^{(t)} \text{ with } \delta\mathbf{V}^{(t)} = \mathbf{N}(0, \Sigma_{C \times M}^{(t)})$$

- Compute the model from  $\mathbf{V}^{(gen)}$

$$x^{(gen)}[n] = \sum_{c=1}^C x_c^{(gen)}[n]$$

- Compute the LS function  $l_{LS}(\mathbf{V}^{(gen)})$

- If  $l_{LS}(\mathbf{V}^{(t)}) - l_{LS}(\mathbf{V}^{(gen)}) > 0$

$$\text{set } \mathbf{V}^{(t+1)} = \mathbf{V}^{(gen)}, l_{LS}(\mathbf{V}^{(t+1)}) = l_{LS}(\mathbf{V}^{(gen)})$$

otherwise **generate a new parameter vector again**

- Draw a random number according to a uniform distribution

$$u \sim U[0,1]$$

- If  $u < 2/3$

$$\text{set } \sigma_{(i)}^{2(t+1)} = (1 - \varepsilon_\sigma) \sigma_{(i)}^{2(t)} \quad \forall i$$

$$\text{otherwise set } \sigma_{(i)}^{2(t+1)} = 1/(1 - \varepsilon_\sigma) \sigma_{(i)}^{2(t)} \quad \forall i$$

- While  $t < iter$

set  $t=t+1$  and **iterate step 2'**

Table 2 – Step 2' of the global algorithm of the Short-LP with an adapted simulating-annealing-based algorithm for a multi-component signal - In this case and compared with step 2 of the monocomponent case, the decrement  $\varepsilon_\sigma$  of the parameter perturbation variance has a default value equal to 0.04 and there is no more temperature parameter.

### 3.2. Sub-optimal Algorithm by deflation

The deflation approach consists of a component-by-component algorithm. At iteration  $c$ , the  $c^{th}$  component only is estimated through a vector we denote  $\widehat{\mathbf{V}}_{\rightarrow c}$ . Instead of the parameter vector  $\mathbf{V}$  defined in (3),  $\widehat{\mathbf{V}}_{\rightarrow c}$ , defined as

$$\widehat{\mathbf{V}}_{\rightarrow c} = \begin{bmatrix} \mathbf{V}_1^T & \dots & \mathbf{V}_{c-1}^T & \widehat{\mathbf{V}}_c^T & \mathbf{0}^T & \dots & \mathbf{0}^T \end{bmatrix}_{(C-c)\text{times}}, \quad (8)$$

with  $\mathbf{0}^T$  the null vector of dimension  $M$  is partially filled in according to the iteration number. For the same reasons as in the previous section, a modified simulated-annealing technique is applied for estimating this vector.

At each iteration  $c$ , the  $c^{th}$  component of  $\widehat{\mathbf{V}}_{\rightarrow c}$  is initialized as in Table 1 but from the Fourier Transform of the residue of the previous iteration.

Table 3 shows the principle of this algorithm. Inside the deflation loop, the iteration step, referred to as **step 2''**, is close to step 2' of Table 2 but for one component only. The perturbation matrix is of dimension  $M$  only.

<b>Inputs</b>	
- $s[n]$	the observation over $[N/2, N/2]$
- $C$	the component number
- $Ma_c$	the orders of the amplitude polynomial for each $c=1, C$ (by default 2)
- $Mf_c$	the order of the frequency polynomial for each $c=1, C$ (by default 2)
- $iter$	the number of iterations (by default 500)
- $\varepsilon_\sigma$	the decrement of the parameter perturbation variance (by default 0.01)
<b>Initialization of the residue</b> $r_1[n] = s[n]$	
<b>Deflation loop - Iterations from <math>c=1, C</math></b>	
<b>Step 1 from Table 1</b> $\rightarrow$ Initialization $\hat{\mathbf{V}}_{\rightarrow c}^{(0)}$ from $FT_c(f)$	
<b>Step 2" - Iterations from <math>t=1, iter</math></b>	
- Generate a new parameter vector deviated from a Gaussian perturbation	
$\mathbf{V}_c^{(gen)} = \mathbf{V}_c^{(t)} + \delta \mathbf{V}_c^{(t)}$ with $\delta \mathbf{V}_c^{(t)} = \mathbf{N}(0, \Sigma_M^{(t)})$	
- Compute the model from $\mathbf{V}_c^{(gen)}$	$x_c^{(gen)}[n] = a_c^{(gen)}[n] \cos(\phi_c^{(gen)}[n])$
- Compute the LS function	$l_{LS}(\mathbf{V}_c^{(gen)})$
- If $l_{LS}(\mathbf{V}_c^{(t)}) - l_{LS}(\mathbf{V}_c^{(gen)}) > 0$	set $\mathbf{V}_c^{(t+1)} = \mathbf{V}_c^{(gen)}$ , $l_{LS}(\mathbf{V}_c^{(t+1)}) = l_{LS}(\mathbf{V}_c^{(gen)})$
	otherwise <b>generate a new parameter vector again</b>
- Draw a random number according to a uniform distribution	$u \sim U[0, 1]$
- If $u < 2/3$	set $\sigma_{(i)}^{2(t+1)} = (1 - \varepsilon_\sigma) \sigma_{(i)}^{2(t)} \quad \forall i$
	otherwise set $\sigma_{(i)}^{2(t+1)} = 1 / (1 - \varepsilon_\sigma) \sigma_{(i)}^{2(t)} \quad \forall i$
- While $t < iter$	$t = t + 1$ and <b>iterate step2"</b>
<b>Step 3 - Construction and deflation of the <math>c^{\text{th}}</math> component</b>	
- Set $\mathbf{V}_c^{(iter)}$ in $\hat{\mathbf{V}}_{\rightarrow c}$	
- Compute $x_c[n]$ from the $c^{\text{th}}$ component of $\hat{\mathbf{V}}_{\rightarrow c}$	
- Deflate this $c^{\text{th}}$ component from the observation	$r_{c+1}[n] = r_c[n] - x_c[n]$
- Until $c < C$	set $c = c + 1$ and iterate the <b>deflation loop</b>
	otherwise set $x[n]$ from $\hat{\mathbf{V}}_C = \hat{\mathbf{V}}_{\rightarrow c}$ and <b>stop the algorithm</b>

Table 3 – The deflation algorithm of the Short-LP with an adapted simulating-annealing-based algorithm for a multi-component signal

## V. FREQUENCY RESOLUTION LIMIT

In this section, the limit of the frequency resolution of the Short-LP is evaluated by means of simulations. A set of signals, referred to as *Testset 1*, is simulated according model (1) with two close quadratic-frequency modulations. In order to break up the influence of the amplitude modulation, the amplitudes of both components are set to the same constant value. The parameter vectors  $\mathbf{V}_c$  as defined in (4) are set up for each component to

$$\begin{aligned} \mathbf{V}_1 &= [16 \quad 0.4 \quad 1.90 - 0.2 - 0.5]^T \text{ with } Ma_1 = 0, Mf_1 = 2 \\ \mathbf{V}_2 &= [16 \quad 1.0 \quad f_{2,0} - 0.2 - 0.5]^T \text{ with } Ma_2 = 0, Mf_2 = 2 \end{aligned} \quad \text{for Testset 1.} \quad (9)$$

$N$  is equal to 32 and the signal to noise ratio is 15 dB. The sampling period is 1s. At each date, the frequency distance between each component is a constant number  $\Delta f$ , which lies in the range  $[0.0870 \text{ Hz}, 0.0087 \text{ Hz}]$ . This distance is set by means of the value of  $f_{2,0}$ , see Table 4. For an easier comparison with Fourier-based method, the last line of Table 4 gives  $\Delta f$  in frequency bins.

$f_{2,0}$ in Hz	1.85	1.80	1.75	1.70	1.65	1.60	1.55	1.50	1.40	1.45
$\Delta f = (f_{1,0} - f_{2,0}) p_0[n]$ in Hz	0.0087	0.0174	0.0261	0.0348	0.0435	0.0522	0.0609	0.0696	0.0783	0.0870
$\Delta f \times (N+1)$ in frequency bins	0.2871	0.5742	0.8613	1.1484	1.4355	1.7226	2.0097	2.2968	2.5839	2.871

Table 4 – Theoretical frequency resolutions of the Testset 1,  $f_{1,0}$  being equal to 1.90 and  $p_0[n]$  to  $\frac{1}{\sqrt{N+1}}$  with  $N=32$  according to the discrete base used. The colour qualifies the results of the Short-LP: red, orange and green for bad, so-so and good respectively.

In the algorithms proposed, the modulation orders are assumed to be unknown. As already specified in section II, we set the modulation orders to the maximum value that is 2.

Figure 1 and Figure 2 show the results for some characteristic values of the frequency distance. Down to a frequency distance equal to 0.06 Hz, the algorithm is able to separate both components with an accurate estimation of the modulation functions. As already mentioned in the statistical study [6], estimating the magnitude is always more difficult especially at low frequencies. Despite this, the time model is close to the theoretical signal as shown by the curves at the top of Figure 1.

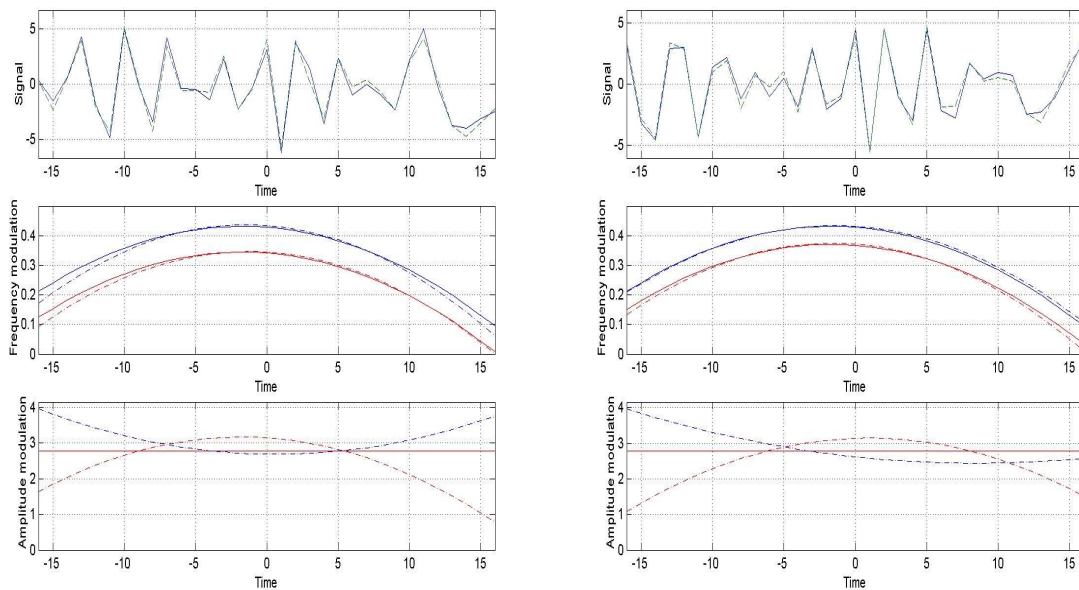


Figure 1 - Good results of Short-LP with Testset 1 for  $\Delta f = 0.087\text{Hz}$  (left) and  $\Delta f = 0.0609\text{Hz}$  (right). Top to bottom, both theoretical (-) and estimate (-): time signal, frequency modulations and amplitude modulations of both components

Then, as illustrated in Figure 2, the algorithm behaves worse for a frequency distance lying in the range [0.03 Hz, 0.06 Hz]. At  $\Delta f = 0.0348\text{Hz}$ , the frequency modulations are properly estimated, whereas the amplitude modulation presents a higher standard deviation. Then, at lower  $\Delta f$ , such as  $\Delta f = 0.0261\text{Hz}$ , one component is estimated at a frequency equal to the frequency mean, the other one with a frequency modulation of any type rather in the low frequencies. Curiously, the modulation errors compensate each other in order that the time model always lies close to the theoretical signal as shown by the curves at the top of Figure 2.

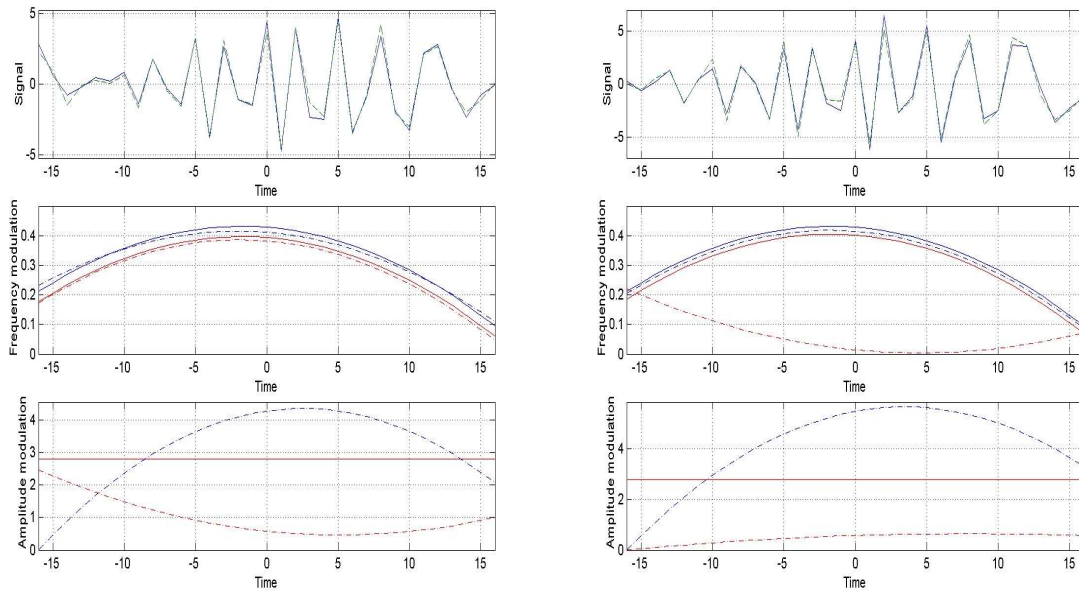


Figure 2 – Results of Short-LP with Testset 1 for  $\Delta f = 0.0348\text{Hz}$  (left) and  $\Delta f = 0.0261\text{Hz}$  (right). Top to bottom, both theoretical (-) and estimate (- -): time signal, frequency and amplitude modulations of both components.

Under 0.03 Hz, this behaviour is accentuated. The algorithm estimates only one component at the mean frequency with amplitude equal to the sum of the two components. Given that the algorithm has one supplementary degree of freedom, the second component is estimated at low frequencies and amplitudes. Even at these frequency distances, the time model always lies close to the theoretical signal. Moreover, the estimation error is the lowest at these frequencies.

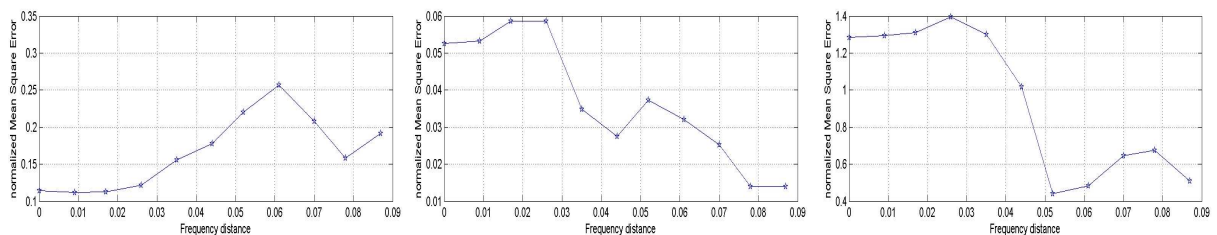


Figure 3 – Mean square error of the time signal (left), frequency modulation (middle) and amplitude modulation (right), normalized by the signal power, of Testset 1 versus the frequency distance between the two components for 100 noise runs.

Figure 3 presents the mean square errors versus the frequency distance and illustrates this behaviour. The three frequency ranges observed experimentally can be also detected on the mean square error evaluated between the time model and the theoretical signal. The error increases whereas the frequency distance decreases until a critical value, 0.0609 Hz, from which the errors decreases again. As expected, the mean square errors between the frequency or the amplitude modulations increase while the frequency distances decrease. In fact, this behaviour can be explained by the fact that the modulation orders are constant in the model. The degrees of freedom of the model permit an accurate modelling of the signal. Moreover, these simulations allow us to conclude that the error

between the model and the observation should not be used as the only stop criterion when the modulation orders are constant. A whiteness criterion should be added.

The critical value 0.0609 Hz equal to 2 bins can be assumed to be the frequency resolution of the algorithm at the given signal to noise ratio (15 dB) and for the given signal length (33 points). The location of the frequency modulation, in the signal frequency band, or the arch back of this modulation have no effect upon the result. We get the same result with a convex frequency modulation (*Testset 2* with  $f_{1,0}=1.2$ ,  $f_{1,1}=f_{2,1}=+0.18$ ,  $f_{1,2}=f_{2,2}=+0.3$  and always  $N$  equal to 32 and the signal to noise ratio to 15 dB).

In order to understand this value according to the theoretical modulation law of the signal, it may be interesting to determine the degree of energy concentration of the signal in the time-frequency plane. Rihaczek [11] has investigated this question by means of a time-frequency cell,  $T_r \times B_d$ , within most of the signal energy is concentrated, and defined as the deviation of the phase from the linearity. The interval  $T_r$ , referred to as the relaxation time, is the time over which the signal phase may be considered linear, or the instantaneous frequency constant. The frequency band  $B_d$ , referred to as the dynamic signal bandwidth, is the frequency band swept during this time. Rihaczek shows that

$$B_d = \sqrt{\frac{1}{2\pi} \frac{df_c(t)}{dt}} = \frac{1}{T_r} \quad (10)$$

with  $f_c(t)$  the instantaneous frequency of the signal. The dynamic bandwidth depends on the rate of change of the instantaneous frequency. For nonlinear modulations the cell size varies with time.

In the case of signals belonging to *Testset 1* defined in (9), Figure 4 shows the variation of  $B_d$ , which lies in the range [0.0253 Hz, 0.1951 Hz]. Consequently,  $T_r$  varies between 5.1s when the modulation rate change is high, and 39.5s at the middle of the window when the modulation rate change is nearly null. The Short-LP frequency model is of order 2, so has no limit in time. In frequency, the Short-LP gives a good indication given that  $B_d$  is almost greater than the frequency resolution limit 0.0609 Hz we observed in simulations. To compare with a classical analysis, a spectrogram with a Hanning window should attain 0.09 Hz only and over 16s, which stands for 2.97 bins of the full signal. Figure 5 should be compared with Figure 1 (right).

These results have been obtained for a signal length of 33 points and at a signal to noise ratio equal to 15 dB. For a longer length and, works in progress seems to corroborate that the critical value of 2 bins could be the resolution limit whatever the length. But further works are required to confirm this assumption and to assess the robustness to the noise level.

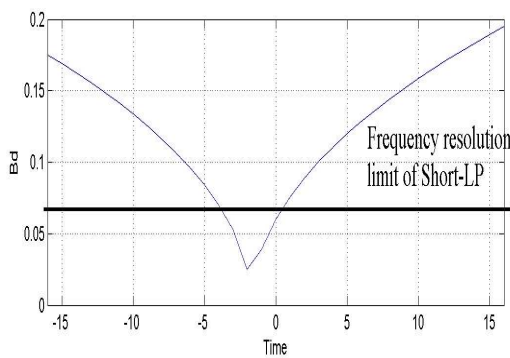


Figure 4 – Dynamic signal bandwidth of the components of *Testset 1* over the time support of 33 s (33 points)

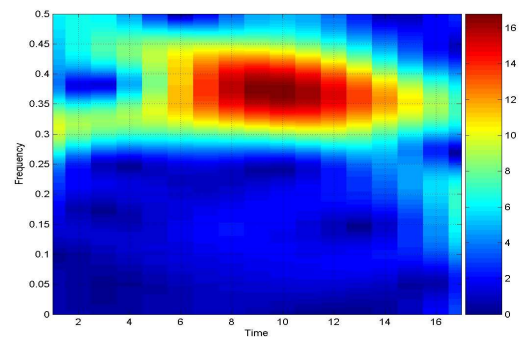


Figure 5 – Spectrogram with a Hanning window of length 16 s (16 points) of *Testset 1* for  $\Delta f = 0.0609\text{Hz}$

## VI. DISCRIMINATION AM VERSUS TWO FMS

In this section we aim at evaluate the behaviour of the algorithm when analysing one component only according to the amplitude modulation properties. Indeed the spectrum of such a signal has two adjacent sidebands. We asked about the behaviour of the algorithm in this case. How many degrees of freedom does the algorithm require? Does the algorithm need one or two components for modelling one AM component? As in the previous section, our conclusions will be drawn from simulations. Two properties have to be considered: First the frequency distance between the two sidebands of the amplitude modulation. Second the sign of the amplitude.

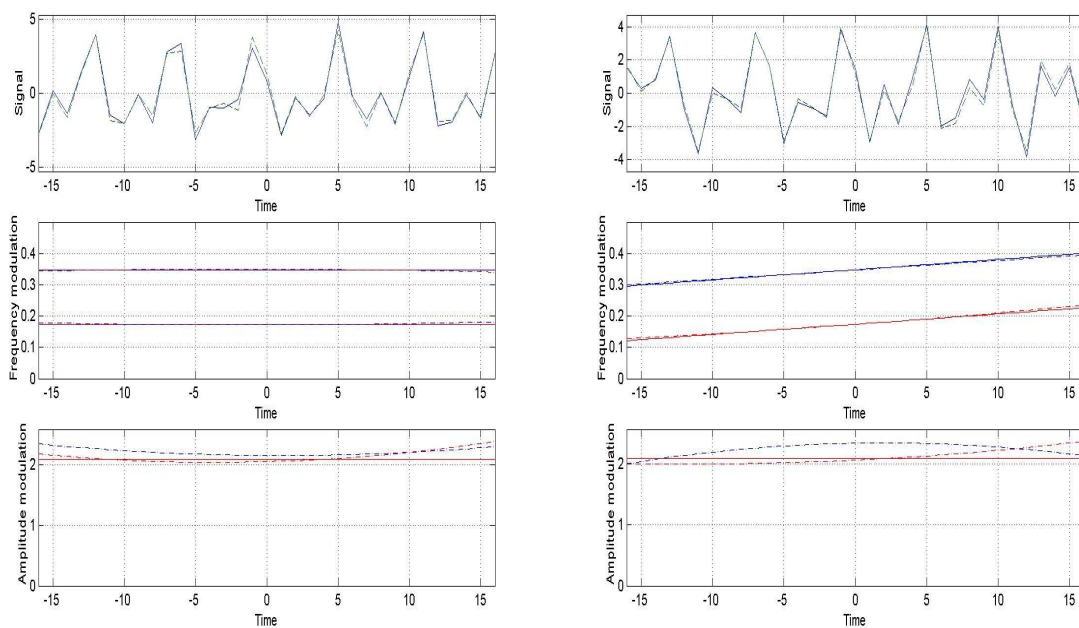


Figure 6 - Results of Short-LP with Testset 3.1 (left) and Testset 3.2 (right), 2 constant and linear FM parallel components ( $\Delta f = 0.1741$  Hz) with constant AM. Top to bottom, both theoretical (-) and estimate (--): time signal, frequency and amplitude modulations of both components.  $C=2$ .

Two testsets, *Testset 3* and *Testset 4* have been considered in order to answer this question, with always  $N$  equal to 32 and the signal to noise ratio to 15 dB. Features of these Testsets and a sum up of the results of the Short-LP are given in Table 5.

When the signal is made of two components and as expected, the Short-LP is not able to model it with one degree of freedom ( $C=1$ ) as shown with *Testset 3.1* and *3.2* in Table 5 and in Figure 6.

When the signal is made of one amplitude-modulated component, the Short-LP will be able to manage whatever the degree of freedom.

	<b>Features of the Testsets</b> 33 points, signal to noise ratio 15 dB FM is for Frequency Modulation AM for Amplitude Modulation	<b>Peak number in the theoretical spectrum</b>	<b>Normalized mean square error of the Short-LP</b>	
			<b>C=2</b>	<b>C=1</b>
<b>Testset 3</b>	1. 2 constant FM parallel components ( $\Delta f = 0.1741$ Hz > 0.0609 Hz) with constant AM	2 peaks	0.1435	0.7042
	2. 2 linear FM parallel components ( $\Delta f = 0.1741$ Hz > 0.0609 Hz) with constant AM	Two spectral patterns with several peaks	0.1186	0.6909
<b>Testset 4</b>	1. 1 constant FM component with positive AM ( $\Delta f_m$ between the two sidebands = $2 \times 0.00727$ Hz = 0,01454 Hz < 0.0609 Hz)	2 sidebands non-resolved by a global Fourier spectrum	0.1389	0.1547
	2. 1 constant FM component with non-positive AM ( $\Delta f_m$ between the two sidebands = $2 \times 0.027$ Hz = 0.054 Hz < 0.0609 Hz)	2 sidebands resolved by a global Fourier spectrum	0.3327	0.6204
	3. 1 linear FM component with positive AM ( $\Delta f_m$ between the two sidebands = $2 \times 0.0058$ Hz = 0.0116 Hz < 0.0609 Hz)	1 spectral pattern with several peaks	0.1061	0.2490
	4. 1 linear FM component with non-positive AM ( $\Delta f_m$ between the two sidebands = $2 \times 0.043$ Hz = 0.0868 Hz > 0.0609 Hz)	2 sidebands resolved by a global Fourier spectrum	0.3279	0.7408
	5. 1 constant FM component with non-positive AM and the carrier ( $\Delta f_m$ between the two sidebands = $2 \times 0.0428$ Hz = 0.0856 Hz > 0.0609 Hz and the difference between the carrier frequency 0,15 Hz and the AM wave frequency 0.0428 Hz = 0.1072 Hz > 0.0609 Hz)	2 sidebands and the carrier peak resolved by a global Fourier spectrum	0.3881	0.6930

Table 5 – Features and mean square error, normalized by the signal power, of Testset 3 et Testset 4 when considering two different degrees of freedom of the Short-LP. The colour qualifies the results: red, orange and green for bad, so-so and good respectively.

But, in this case, the sign of the amplitude is essential. We assumed that the model in (1) should have positive amplitude in order to maintain the uniqueness of the solution. This constraint can be a limitation in some cases. When the amplitude is positive, see *Testset 4.1* and *4.3* in Table 5 and Figure 7, the Short-LP provides a good model, more accurate with  $C = 1$  in opposition to the error values as already specified in the previous section. When  $C=2$ , given that the frequency distance between the two sidebands, referred as to  $\Delta f_m$ , are lower than the frequency resolution, the Short-LP models the carrier frequency transferring the modulation in the amplitude. The other component is estimated with any frequency modulation and zero-amplitude modulation.

When the amplitude is negative as in *Testset 4.2*, *4.2* and *4.5* of Table 5 and as shown in Figure 8, the Short-LP will produce a better approximation with the highest degree of freedom. However and as expected, the amplitude modulation cannot be tracked in the negative parts and so the normalized mean square error is high whatever the degree of freedom.

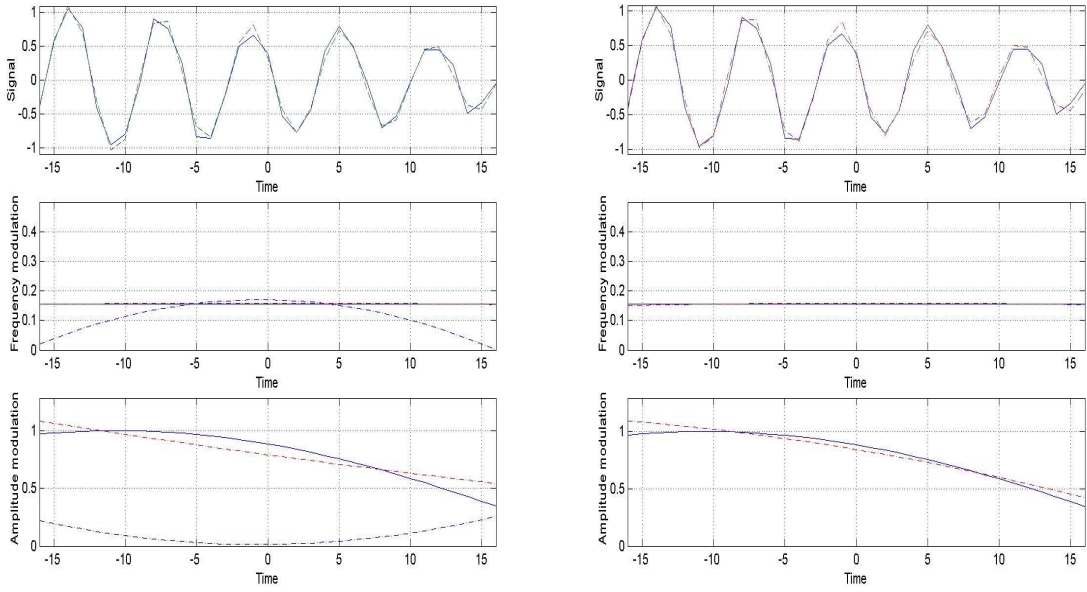


Figure 7 - Results of Short-LP with Testset 4.1, 1 constant FM component with positive AM, with  $C=2$  (left) and  $C=1$  (right). Top to bottom, both theoretical (-) and estimate (--): time signal, frequency and amplitude modulations of both components.

If the modulation index is high as it was the case in the last example, *Testset 4.5* of Table 5, the model has to be applied on shorter parts of the signal and the extension of the algorithm proposed in [4], [8] should be applied.

In conclusion, the simulations tend to show that an amplitude-modulated component with a positive amplitude will be better estimated with a right degree of freedom, that is  $C=1$ . The normalized mean square error does not reflect this accurate modeling given that a higher degree-of-freedom model allows a diminution of the error thanks to a second component. Nevertheless the amplitude modulation and the frequency modulation of the component considered is closer to the theoretical one with  $C=1$ .

Let us try to explain this behaviour. Indeed the positivity constraint on the amplitude corresponds to a signal with a time duration  $T$  that has to be shorter than half the period of the amplitude modulation for retaining the positive part of the modulation only,

$$T < \frac{(2/\Delta f_m)}{2} = \frac{1}{\Delta f_m}. \quad (11)$$

with  $\Delta f_m$  being twice the frequency of the amplitude modulation. However, if we admit that the frequency resolution of the Short-LP is about 2 bins, that is the conclusion of the simulation study of section V, a model with a frequency resolution higher than this limit should verify

$$\Delta f > \frac{2}{T} \Leftrightarrow T > \frac{2}{\Delta f} \quad (12)$$

It is straightforward to conclude that constraints (11) and (12) do not match. Then setting positive amplitude necessarily leads to a frequency distance between the two sidebands,  $\Delta f_m$ , which is lower than the frequency resolution of the method. A model with one degree of freedom is then the best

one. We have not simulated the case with a carrier frequency, which should need a higher degree of freedom.

In the case of non-positive amplitude, the frequency distance between the two spectral sidebands can be either lower or higher than the frequency resolution, and in both cases, the model is not appropriate. A higher degree of freedom allows a better approximation. The model obtained can be quite good but the amplitude modulation will never be correct. The frequency modulations are close to the sidebands of the modulation.

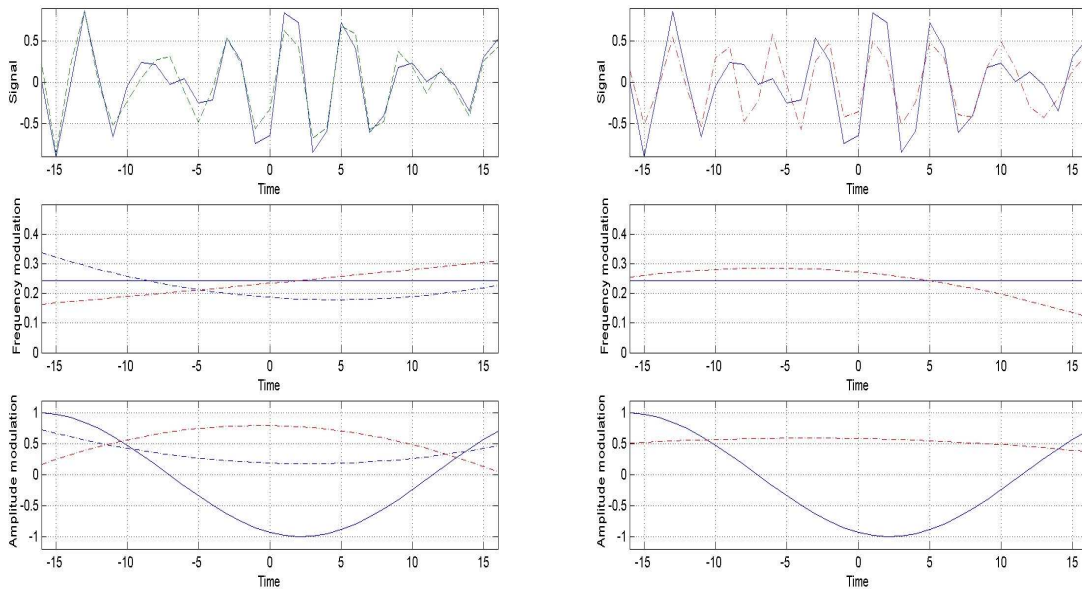


Figure 8 – Results of Short-LP with Testset 4.2, 1 constant FM component with non-positive AM, with  $C=2$  (left) and  $C=1$  (right). Top to bottom, both theoretical (-) and estimate (-): time signal, frequency and amplitude modulations of both components.

## VII. PRIOR UPON FREQUENCY MODULATION

In the foregoing examples the amplitude modulation turns out to be the most difficult part of the Short-LP as in all model-based methods. However, the frequency modulation can be known in some particular applications. For instance, in mechanical systems such as turbines or gearboxes, time variations of the instantaneous frequency can be known *a priori* or estimated from independent synchronous measurements provided by tachometers. Assuming no error in this frequency estimation, this section aims at investigating the properties of the Short-LP for the estimation of the amplitude only, a crucial point in most applications.

*Testset 5* is made of two components with two quadratic-frequency modulation components, each with a quadratic-amplitude modulation. The frequency modulations are known and are set in the initialization step of the algorithm. The amplitude modulations cross each other over the time duration of the signal. The Short-LP is then investigated according to the signal to noise ratio.

Figure 9 shows the result of the amplitude estimation averaged over 50 runs of an additive white noise for a signal to noise ratio equal to 15 dB and 5 dB. The exact frequency modulation is given just for information. At 15 dB the estimation of the amplitude estimation is accurate whereas a little bias appears at 5 dB. Table 6 shows the values of the mean square errors without and with *a priori*

information on the frequency modulation. First and as already visible in Figure 3, the error comes essentially from the amplitude estimation. Second, when the frequency modulation is known, the error can come only from the amplitude estimation and is lower than in the previous case: 0.1685 instead of 0.8254 at 15 dB. The difference is really noticeable.

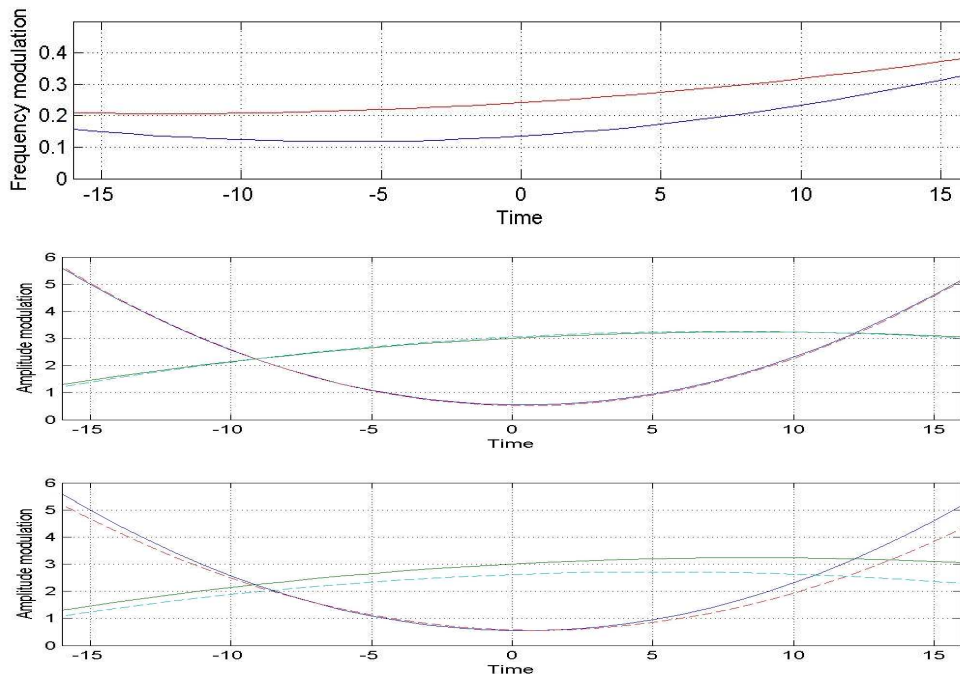


Figure 9 – Results of short-LP with Testset 5, two quadratic frequency and amplitude modulation with a priori known frequency modulation (top). Both theoretical(-) and mean estimate (--) amplitude modulation over 50 runs of an additive white noise with a signal to noise ratio equal to 15 dB (middle) and 5dB (bottom).

Normalized mean square error of the Short-LP	15 dB		5 dB	
	Estimated FM	A priori known FM	Estimated FM	A priori known FM
Time signal	0.2338	0.1648	0.3870	0.5087
Amplitude modulation	0.8254	0.1685	0.8074	0.6089
Frequency modulation	0.0540	0	0.0533	0

Table 6 - Mean square error of the time signal and the amplitude modulation, normalized by the signal power, of Testset 5 at two signal to noise ratio.

Figure 10 shows the normalized mean square errors for a signal to noise ratio lying in the range 0 to 20 dB. The behavior of the Short-LP is nearly linear according to the variation of the signal to noise ratio.

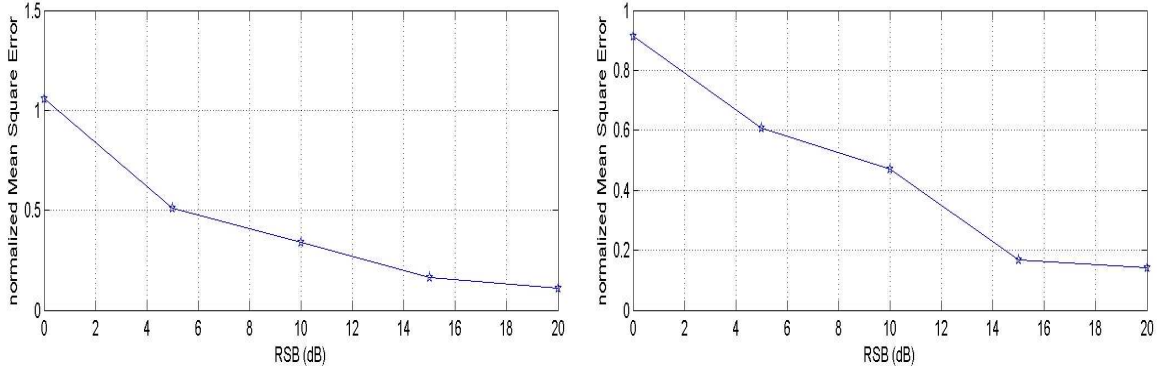


Figure 10 - Mean square error of the time signal (left) and of the amplitude modulation (right), normalized by the signal power, of Testset 5 versus the signal to noise ratio for 50 noise runs.

## VIII. CONCLUSIONS

This paper focuses on some important properties of the Short-LP method previously published by the authors. The Short-LP method estimates all the parameters of a time model, which provides an accurate description of a measured signal. The signals under consideration are multicomponents, nonlinear, nonstationary, and have short duration.

A first set of signal-test allows us to give an approximation of the frequency resolution, which seems to be equal to 2 bins, without forgetting that the signal is nonstationary and nonlinear over a short time duration. The Short-LP is then over performing the Fourier-based method. Further works are in progress for validating this results according the length the signal and the signal to noise ratio. We also attempt to explain the value obtained according to the dynamic signal bandwidth, the signal being nonstationary.

A second set of signal-test explains the number of degrees of freedom necessary for modelling one amplitude-modulation signal. Indeed, the constraint of positive amplitude set by the model definition guides the behaviour of the algorithm. This constraint induces that the amplitude modulation frequency is lower than the frequency resolution of the Short-LP and then the optimal model is a one-component model. If the amplitude is not positive the model is not optimal and the signal is better approximated by a higher degree of freedom. Increasing the degree of freedom will improve the time approximation but non necessarily the frequency and amplitude modulation.

A third set of signal-test shows that an *a priori* knowledge of the frequency modulations, as it is possible in mechanical systems, allows the Short-LP method to reach higher performance for the amplitude estimation.

## Appendix: Expression of the discrete base

In [3] we derived the base  $\{p_m[n]\}_{m=0, \max(Ma_c, Ma_f)}$  used in the Short-LP model,

$$p_0[n] = \frac{1}{\sqrt{N+1}} \quad p_1[n] = \frac{2\sqrt{3}}{\sqrt{N(N+1)(N+2)}} \quad p_2[n] = \frac{6\sqrt{5}}{\sqrt{(N+3)(N+2)(N+1)N(N-1)}} \left( n^2 - \frac{N(N+2)}{12} \right), \quad (13)$$

with  $n = -N/2, N/2$  and for  $Ma_c$  and  $Ma_f$  being equal to 2.

## References

1. M. Aburdene. *On the computation of discrete Legendre polynomial coefficients*, in: *Multidimensional systems and signal processing*. Kluwer Academic Publishers, Boston. Manufactured in The Netherlands, 1993, pp. 181–186.
2. L. Cohen, P. Loughlin and D. Vakman. On an ambiguity in the definition of the amplitude and phase of a signal. *Signal Processing*, Vol. 79, 1999, pp. 301-307.
3. M. Jabloun, F. Leonard, M. Vieira and N. Martin. *Estimation of the Amplitude and the Frequency of Nonstationary Short-time Signals*. *Signal Processing*. Vol. 88, Issue 7, July 2008, pp 1636-1655.
4. M. Jabloun, F. Leonard, M. Vieira And N. Martin. *A New Flexible Approach to Estimate Highly Nonstationary Signals of Long Time Duration*. *IEEE Transactions on Signal Processing*, Vol.55, No.7, July 2007.
5. M. Jabloun, N. Martin, Invited Conference, *On The Modeling And Estimation Of Nonlinear Instantaneous Frequency And Amplitude Of Non-Stationary Signals*. 5th Workshop on Advanced Control and Diagnosis Organized by IAR ICD Working Group, Grenoble, France, November 15-16, 2007.
6. M. Jabloun, N. Martin, M. Vieira, and F. Leonard, *Maximum Likelihood Parameter Estimation Of Short-Time Multicomponent Signals With Nonlinear Am/Fm Modulation*, *IEEE Workshop on Statistical Signal Processing, SSP 05*, Bordeaux, France, July 17 - 20, 2005.
7. M. Jabloun, N. Martin, M. Vieira, and F. Leonard, *Multicomponent Signal: Local Analysis And Estimation*, *EUropean SIgnal Processing Conference, EUSIPCO 05*, Antalya, Turkey, September 4-8, 2005.
8. M. Jabloun, M. Vieira, N. Martin, F. Leonard. *A AM/FM Single Component Signal Reconstruction using a Nonsequential Time Segmentation and Polynomial Modeling*. *International Workshop on Nonlinear Signal and Image Processing, NSIP 2005*, Sapporo Convention Center, Sapporo, Japan, May 18-20, 2005.
9. M. Jabloun, M. Vieira, N. Martin and F. Léonard. *Local orthonormal polynomial decomposition for both instantaneous amplitude and frequency of highly non-stationary discrete signals*. *Sixth International Conference on Mathematics in Signal Processing, IMA 2004*, Royal Agricultural College, Cirencester, UK, 14-16 December 2004.
10. P.L. Loughlin and B. Tacer. *On the amplitude-and frequency-modulation decomposition of signals*. *Journal of Acoustical Society of America*, Vol.100, n°3, September 1996, pp. 1594-1601.
11. A.W. Rihaczek, *Signal Energy distribution in time and frequency*. *IEEE Trans. On Information Theory*, Vol. 14, n°3, May 1968, pp. 369-374.